Open access • Journal Article • DOI:10.1021/NL400738P

Sliding-Triboelectric Nanogenerators Based on In-Plane Charge- Separation Mechanism — Source link

Sihong Wang, Long Lin, Yannan Xie, Qingshen Jing ...+3 more authors

Institutions: Georgia Institute of Technology, Chinese Academy of Sciences

Published on: 12 Apr 2013 - Nano Letters (Nano Lett)

Topics: Triboelectric effect and Electrostatic induction

NANO LETTERS

Letter

pubs.acs.org/NanoLett

Sliding-Triboelectric Nanogenerators Based on In-Plane Charge-Separation Mechanism

Sihong Wang,[†,#] Long Lin,[†,#] Yannan Xie,[†] Qingshen Jing,[†] Simiao Niu,[†] and Zhong Lin Wang*[,†,‡]

[†]School of Materials Science and Engineering, Georgia Institute of Technology, Atlanta, Georgia 30332-0245, United States

[‡]Beijing Institute of Nanoenergy and Nanosystems, Chinese Academy of Sciences, Beijing, China

S *Supporting Information*

ABSTRACT: Aiming at harvesting ambient mechanical energy for self-powered systems, triboelectric nanogenerators (TENGs) have been recently developed as a highly efficient, cost-effective and robust approach to generate electricity from mechanical movements and vibrations on the basis of the coupling between triboelectrification and electrostatic induction. However, all of the previously demonstrated TENGs are based on vertical separation of triboelectric-charged planes, which requires sophisticated device structures to ensure enough resilience for the charge separation, otherwise there is no output current. In this paper, we demonstrated a newly designed TENG based on an in-plane charge separation process using the relative sliding between two contacting surfaces. Using Polyamide 6,6 (Nylon) and polytetrafluoroethylene (PTFE) films with surface etched nanowires, the two polymers at the opposite ends of the triboelectric series, the newly invented TENG produces an open-circuit voltage up to ~1300 V and a short-circuit current density of 4.1 mA/m^2 with a peak power density of 5.3 W/m^2, which can be used as a direct power source for instantaneously driving hundreds of serially connected light-emitting diodes (LEDs). The working principle and the relationships between electrical outputs and the sliding motion are fully elaborated and systematically studied, providing a new mode of TENGs with diverse applications. Compared to the existing vertical-touching based TENGs, this planar-sliding TENG has a high efficiency, easy fabrication, and suitability for many types of mechanical triggering. Furthermore, with the relationship between the electrical output and the sliding motion being calibrated, the sliding-based TENG could potentially be used as a self-powered displacement/speed/acceleration sensor.

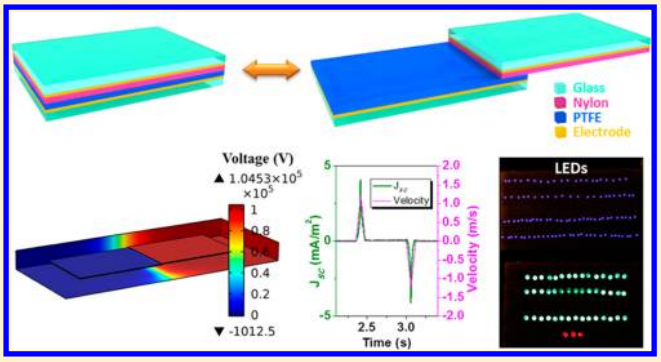

KEYWORDS: *Mechanical energy harvesting, triboelectric nanogenerators, in-plane charge separation, self-powered systems*

The fundamental science and practical applicable technologies for harvesting ambient environmental energy[1−6] are not only essential in realizing the self-powered electronic devices and systems[7,8] but also tremendously helpful in meeting the rapid-growing worldwide energy consumptions. Mechanical energy is one of the most universally existing, diversely presenting but usually wasted energies in the natural environment, which has attracted a lot of effort in developing the energy harvesting techniques based on different effects and mechanisms, such as electrostatics,[9,10] piezoelectricity,[11−13] and electromagnetics.[14,15] The triboelectric effect[16,17] is a well-known phenomenon that can generate electrostatic charges from mechanical contact. However, it has always been deemed as an undesirable effect for electronic systems. The recent invention of triboelectric nanogenerators (TENGs) has made use of this effect to generate electricity through scavenging mechanical energy, which is proven to be extremely efficient, reliable and cost-effective.[18−21] This type of nanogenerator is based on the coupling between triboelectrification and electrostatic induction: the periodic separation between surfaces with opposite triboelectric charges (tribo-charges) can change the induced potential difference between two electrodes to drive the alternating flow of electrons through an external load.[20,22] The previously demonstrated TENGs are all based on the vertical separation of two triboelectrically charged (tribo-charged) planes to generate the electric polarization/field in the direction perpendicular to the planes.[18−24] To realize such vertical charge separation, an air gap is mandatory to be created after the releasing of the external force, which usually requires sophisticated design of the device structures and makes the TENG difficult for packaging and practical use for some cases.

In this study, we demonstrated a new TENG that is designed based on the in-plane sliding between the two surfaces in lateral direction. With an intensive triboelectrification facilitated by sliding friction, a periodic change in the contact area between two surfaces leads to a lateral separation of the charge centers, which creates a voltage drop for driving the flow of electrons in

Received: February 27, 2013
Revised: March 28, 2013
Published: April 12, 2013

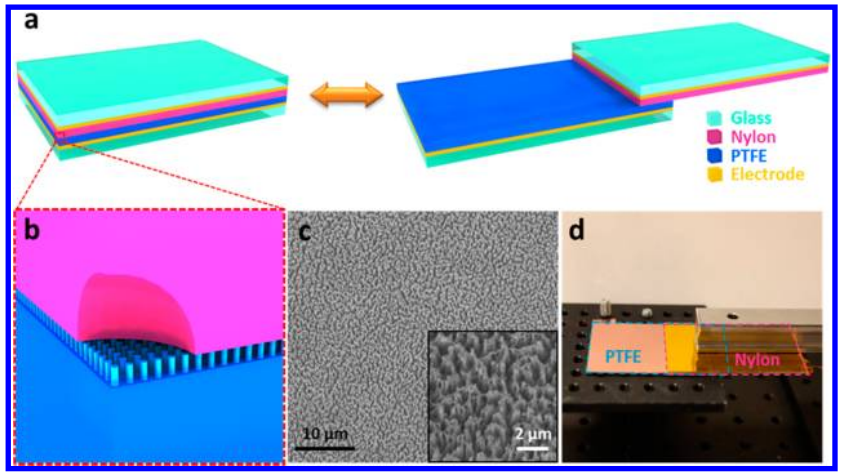

Figure 1. Device structure of a sliding-triboelectric nanogenerator (TENG). (a) The schematic diagram showing the structural design of the TENG in two sliding states: the overlapping position (on the left) and the separation position (on the right). (b) The magnified schematic of the surface between the two polymeric films, showing the fabricated nanowire array on PTFE surface. (c) SEM image of the PTFE surface with etched nanowire structure at the tilted view of 30°, the inset is the SEM image in higher magnification. (d) The photograph of a typical sliding-driven TENG on the measurement stage.

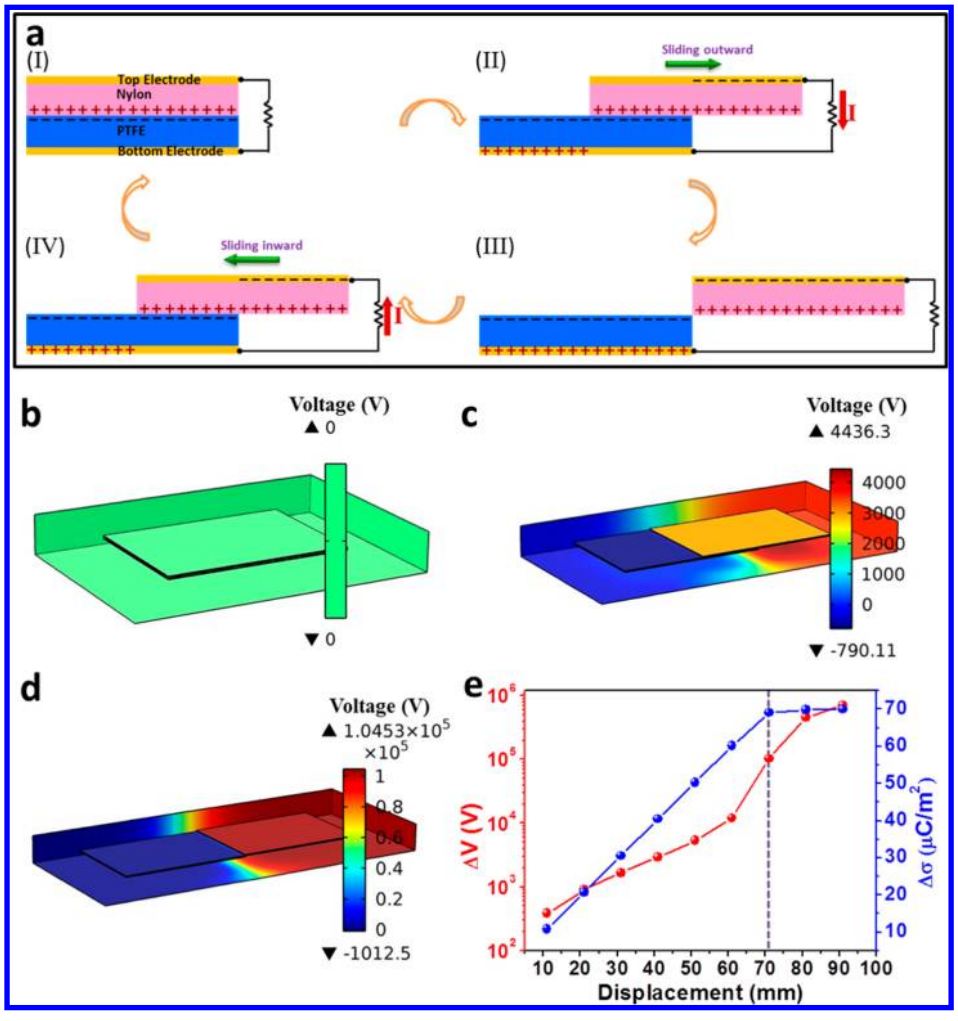

Figure 2. Working mechanism of the TENG based on in-plane charge separation. (a) The sketches that illustrate the electricity generation process in a full cycle of the sliding motion. (b–d) Finite element simulation of the potential difference between the two electrodes at consecutive sliding displacements: (b) 0 mm (the overlapping position); (c) 41 mm (sliding half way out); and (d) 71 mm (fully sliding out). (e) The curves of the simulated potential difference ΔV (red) and transferred charge density $\Delta\sigma$ (blue) versus the sliding displacement from 11 to 91 mm in which the two plates fully slide out of each other at 71 mm (marked by the purple dot line).

dx.doi.org/10.1021/nl400738p | *Nano Lett.* 2013, 13, 2226–2233

the external load. With the help of finite-element simulation, the working principle has been elaborated. Under this new working mode, the open-circuit voltage of the sliding-TENG reaches 1300 V with a peak short-circuit current density of 4.1 mA/m^2 and a peak power density of 5.3 W/m^2, which is capable to drive hundreds of electronic devices (such as LEDs) instantaneously. In this demonstration of the in-plane charge separation based TENG, we systematically studied the influence of the sliding parameters (the displacement and the velocity) on the electrical outputs, which illuminated the distinct characteristics of the TENGs in this new working mode. This work will open up a new category of TENGs with numerous advantages and potential applications of harvesting different types of naturally existing mechanical energies, as well as active sensors.

The sliding-triboelectric nanogenerator is structurally composed of two plates (71 mm × 50 mm) with glass slides as the supporting substrates to ensure the surface flatness (Figure 1a). Polyamide 6,6 (Nylon) and polytetrafluoroethylene (PTFE) films, the two polymers at the opposite ends of the triboelectric series,[25] are purposely chosen as the triboelectric layers adhered on surfaces of the glass slides, respectively, for effective electrification during sliding. On each polymer film, a layer of metal electrode was deposited on the side next to the glass slide (named as top electrode for the one on Nylon and bottom electrode for the one on PTFE). The two plates are kept in parallel to each other and the polymeric surfaces are in intimate contact. As driven by the mechanical motion/vibration along the long-edge of the plate, the two plates slide against each other with the contact area changing periodically. In order to enhance the triboelectric charge density on the surface,[18,22] the PTFE film was dry-etched using inductively coupled plasma (ICP) to create aligned nanowire structures[26] (Figure 1b), which will increase the surface roughness and the effective surface area. As shown in the scanning electron microscopy (SEM) images (Figure 1c), the PTFE surface is uniformly covered with nanowire-structures with an average length of ~1.5 μm. As illustrated in Figure 1d, during the real-time measurement the PTFE-covered plate was bonded to a stationary stage, while the Nylon side was fastened to a parallel flat-end rail guide, which was connected to a linear motor for inducing an in-plane sliding motion.

The sliding-induced electricity generation mechanism is schematically depicted in Figure 2a. In the original position (Figure 2a-I), the two polymeric surfaces fully overlap and intimately contact with each other. Because of the large difference in the ability to attract electrons, the tribo-electrification will leave the Nylon surface with net positive charges and the PTFE with net negative charges with equal density. Since the tribo-charges on the insulators will only distribute in the surface layer and will not be leaked out for an extended period of time,[27] the separation between the positively charged surface and negatively charged surface is negligible at this overlapping position, and thus there will be little electric potential drop across the two electrodes. Once the top plate with the positively charged surface starts to slide outward (Figure 2a-II), the in-plane charge separation is initiated due to the decrease in contact surface area. The separated charges will generate an electric field pointing from the right to the left almost parallel to the plates, inducing a higher potential at the top electrode. This potential difference will drive a current flow from the top electrode to the bottom electrode in order to generate an electric potential drop that cancels the tribo-charge-induced potential. Because the vertical distance between the electrode layer and the tribo-charged polymeric surface is negligible compared to the lateral charge separation distance, the amount of the transferred charges on the electrodes approximately equals the amount of the separated charges at any sliding displacement. Thus, the current flow will continue with the continuation of the ongoing sliding process that keeps increasing the separated charges until the top plate fully slides out of the bottom plate and the tribo-charged surfaces are entirely separated (Figure 2a-III). The measured current should be determined by the rate at which the two plates are being slid apart.

Subsequently, when the top plate is reverted to slide backward (Figure 2a-IV), the separated charges begins to get in contact again but no annihilation due to the insulator nature of the polymer materials. The redundant transferred charges on the electrodes will flow back through the external load with the increase of the contact area in order to keep the electrostatic equilibrium. This will contribute to a current flow from the bottom electrode to the top electrode along with the second half cycle of sliding. Once the two plates reach the overlapping position, the charged surfaces get into fully contact again. There will be no transferred charges left on the electrode, and the device returns to the state in Figure 2a-I. In this entire cycle, the processes of sliding outward and inward are symmetric, so a pair of symmetric alternating current peaks should be expected.

This in-plane charge-separation-induced potential difference and charge transfer can be verified through numerical simulation using COMSOL. The model constructed here has the same structure and dimensions (71 mm × 50 mm in surface) with the real device, and those two tribo-charged surfaces are assigned with a charge density of ± 70 $\mu C/m^2$, respectively. The device is in open-circuit condition, which means no electron transfer between the two electrodes. As shown by the simulation results, when the two plates are in the fully aligned stacking position, which corresponds to the state in Figure 2a-I, there is no potential difference generated (Figure 2b). When the top plate slides about halfway out (with a displacement of 41 mm), there will be a 2950 V potential difference between the two electrodes (Figure 2c); this potential difference will increase to 1.03×10^5 V when the top plate just slides out of touching the bottom plate (with a displacement of 71 mm) (Figure 2d). In these simulation results of Figure 2b–d, the background planes show the potential distribution in the free space of air surrounding the TENG, as a result of the in-plane charge separation. We have also simulated the voltage between the two electrodes at a series of displacements from 11 to 91 mm (with the sketches of the simulated voltage distributions displayed in Figure S1 in the Supporting Information). As shown in Figure 2e, the voltage keeps increasing when the displacement gets larger, even after the plates slide out of each other. This is because the voltage is the path-integral of the electric field along the displacement. On the other hand, the amounts of transferred charges between the two electrodes under these different displacements are also simulated through equating the potential of the electrodes at the short-circuit condition. As shown in Figure 2e, the amount of transferred charges increases linearly with the displacement before the top plate slides out of the bottom plate (with the displacement smaller than 71 mm). But different from the trend of the voltage, the amount of transferred charges will saturate at the total amount of tribo-charges on one surface after the plates have fully slid out of each other, because there is no further

dx.doi.org/10.1021/nl400738p | Nano Lett. 2013, 13, 2226–2233

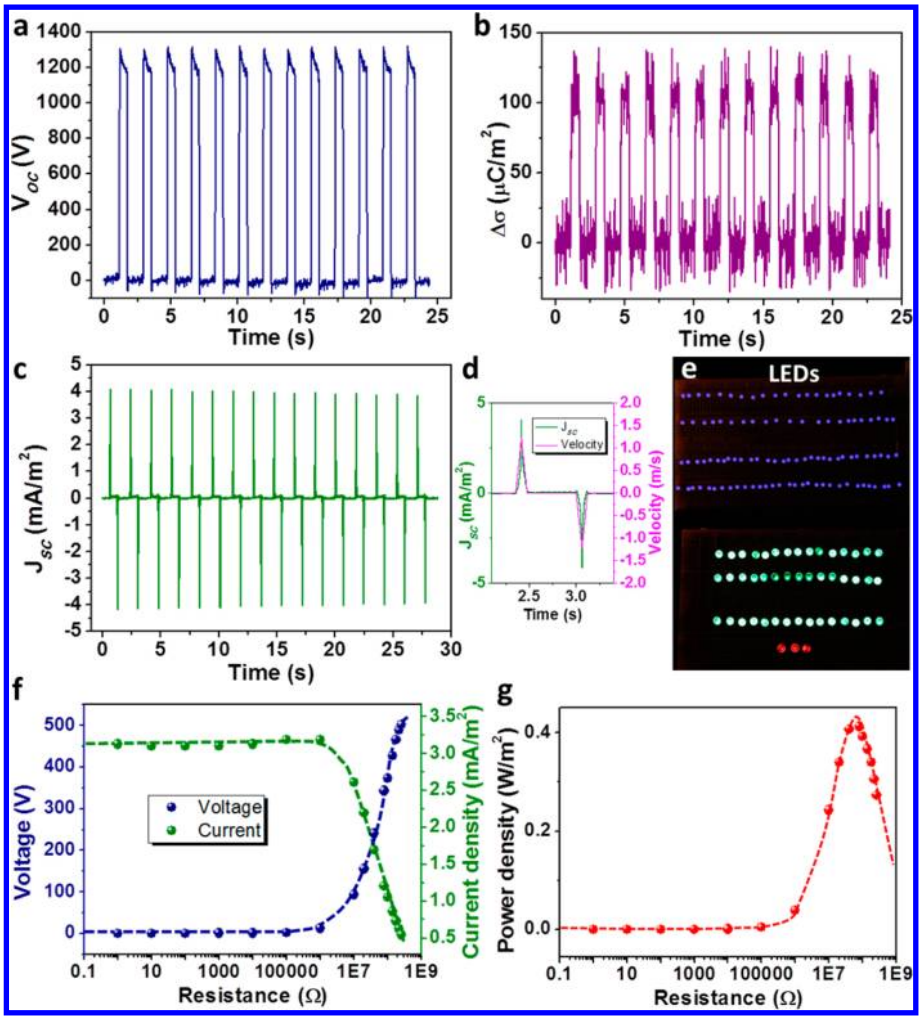

Figure 3. Performance of the TENG driven by the cycled sliding motion. (a) The open-circuit voltage (V_{OC}), (b) the density of transferred charges ($\Delta\sigma$), and (c) the short-circuit current density (J_{SC}) under the in-plane sliding with the displacement of 71 mm and the acceleration of 20 m/s^2. (d) The enlarged profile of J_{SC} within one cycle (green curve) with the corresponding curve of the instantaneous sliding velocity (pink). (e) The snapshot of ~160 commercial LEDs in serial-connection directly driven by a TENG under sliding. (f,g) The dependence of (f) the output voltage (blue) and current density (green) and (g) the power density on the resistance of the external load.

charge separation here. So, the effective displacement region for generating electricity is between 0 and 71 mm, where the contact area of the two plates is changed during the relative sliding of the two plates.

The electrical output of the sliding-TENG was measured with one plate guided by the linear motor in the direction parallel to the long-edge of the plates. The sliding displacement was 71 mm, which was the same with the length of the plate and thus covered the entire effective region for generating electricity (as mentioned above). The sliding movement was in a symmetric acceleration−deceleration mode (the instantaneous sliding velocity was plotted as the pink curve of Figure 3d), with the acceleration rate of ±20 m/s^2. The open-circuit voltage (V_{OC}) was measured by an electrometer with very large input resistance. The electrode at the back of Nylon film was connected to the positive probe. When the plates in the TENG slid from the contact position to the separated position, the V_{OC} jumped from 0 to ~1300 V (Figure 3a), which reflects the induced potential difference between the two electrodes by the in-plane charge separation. At the separation position, the V_{OC} decayed a little bit due to the slow charge leakage through the electrometer. When the TENG slid back to the contact position, the V_{OC} jumped back to 0. The density of the transferred charge ($\Delta\sigma$) was also measured at the short-circuit condition. As shown in Figure 3b, the charges with a density of ~105 μC/m^2 transferred back and forth between the two electrodes, while the plates slid in and out. Since the plates got fully separated in each cycle, the transferred charge density should approximately equal to the triboelectric charge density on the polymeric surfaces, according to the relationship in Figure 2e. With these experimental results, the measured V_{OC} is smaller than the simulated potential difference in Figure 2d, which is possibly due to the limitation of the electrical measurement system to record such a high voltage and the imperfection from the ideal open-circuit condition. The transfer of the charges between the electrodes in the outer circuits produced an alternating-current output with the peak short-circuit current density (J_{SC}) of 4.1 mA/m^2 at a maximum sliding velocity of 1.2 m/s (Figure 3c). The area under each current density peak is the amount of charge density transferred in each sliding motion. The enlarged J_{SC} curve in one single cycle is displayed in Figure 3d, together with the corresponding curve of the sliding velocity. We can find that the current output has a symmetric profile and synchronizes very well with

dx.doi.org/10.1021/nl400738p | Nano Lett. 2013, 13, 2226−2233

the velocity of the sliding motion. With such a power output converted from the sliding motion, hundreds of commercial light-emitting diodes (LEDs) can be instantaneously driven by a single TENG device (Figure 3e and Supporting Information Video S1−2).

In practice, the TENG's effective output power to the loads depends on the match with the resistance of the load. As shown in Figure 3f, when the resistance is below ∼1 MΩ, the output current density and the voltage have little changes from the short-circuit condition: the current density remains at a value of J_{SC} while the voltage stays close to 0. This is because the TENG has infinitely large inner resistance. When the resistance goes beyond 1 MΩ, the current density will drop with the increase of the resistance; while the voltage on the load rises up. Consequently, the instantaneous power density on the load (Figure 3g) remains close to 0 with the resistance below 1 MΩ and reaches the maximum value of 0.42 W/m^2 at a resistance of ∼50 MΩ. This is the maximum output power density on the device.

The output of the planar-sliding-driven TENG is directly determined by the parameters of the sliding motion (the displacement and the velocity), because the flow of electricity originates from the tribo-charge separation under sliding. As simulated in Figure 2e, before the two plates fully slide out of each other (with a displacement smaller than 71 mm) the voltage increases monotonically with the displacement. Also, if we assume a uniform tribo-charge distribution on the polymeric surface, the total amount of transferred charges will have a linear relationship with the displacement, which can be expressed in charge density as

$$\frac{\Delta\sigma}{\sigma_0} = \frac{\Delta L}{L_0} \tag{1}$$

where $\Delta\sigma$ is the transferred charge density, σ_0 is the tribo-charge density on the polymeric surface, ΔL is the sliding displacement, and L_0 is the length of the plate which is 71 mm. According to the definition of current density (J), it has the following relationship

$$J = \frac{\mathrm{d}\Delta\sigma}{\mathrm{d}t} \tag{2}$$

where t is the time. After merging eq 1 into eq 2, we will have

$$J = \frac{\sigma_0}{L_0}\frac{\mathrm{d}\Delta L}{\mathrm{d}t} = \frac{\sigma_0}{L_0}v \tag{3}$$

where v is the instantaneous velocity of the sliding. So, the current density should be proportional to the instantaneous velocity at which the two plates are being separated.

A systematic study of these relationships between the electrical outputs (V_{OC} and J_{SC}) and the sliding conditions was carried out experimentally. In the first group of experiments, the electrical outputs were measured under a series of 7 different sliding displacements from 11 to 71 mm with an acceleration kept at 20 m/s^2. As shown in Figure 4a, the V_{OC} increases with the displacement, which is in accordance with the simulation results in Figure 2e. And the measured transferred charge density $\Delta\sigma$ displays a linear relationship with the displacement (the inset of Figure 4b), which can be linearly fitted with the correlation coefficient of 0.981. As for the peak value of J_{SC}, which is in proportional to the maximum velocity v_m, it also has a positive correlation with the displacement

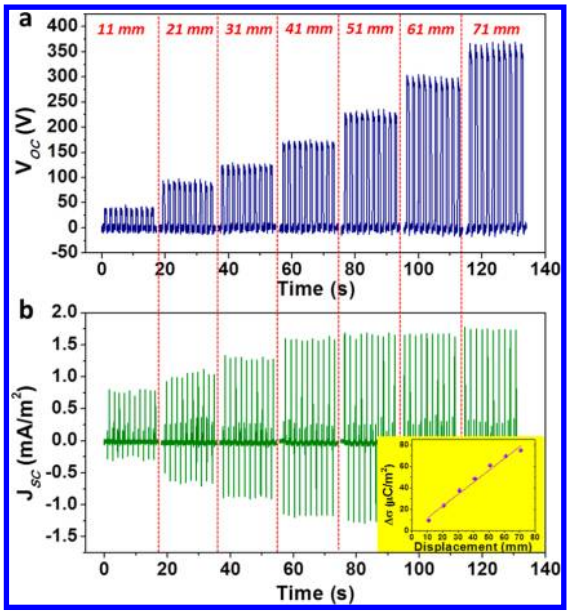

Figure 4. Influence of the sliding displacement on the electrical outputs. (a) The open-circuit voltage (V_{OC}), (b) the short-circuit current density (J_{SC}), and the measured transferred charge density ($\Delta\sigma$) (the inset of b) under 7 different sliding displacements from 11 to 71 mm.

(Figure 4b). This is because v_m has such a relationship with the displacement

$$v_m = \sqrt{a\Delta L} \tag{4}$$

where a is the acceleration and ΔL is the total displacement (the displacement for each acceleration and deceleration process is $\Delta L/2$, respectively).

When the sliding displacement remains at a constant value of 71 mm, the maximum velocity of the sliding is solely determined by the acceleration. Thus, we varied the acceleration to investigate the velocity's influence on the output. As shown in Figure 5a, V_{OC} has very little increase with the rising acceleration, which is also consistent with the theoretical expectation that V_{OC} is only determined by the displacement. However, the changing rate of the voltage will depend on the sliding velocity. The higher the velocity, the faster the voltage increases/decreases in sliding (Figure S2 in the Supporting Information). Through differentiating the curve of V_{OC}−t, the maximum slopes of voltage at the rising edges is plotted with the corresponding maximum sliding velocity in Figure 5b, which shows a clear positive correlation. As for the output current, the peak value of J_{SC} gets larger at higher acceleration, because of the larger maximum velocity in sliding (Figure 5c). However, the sliding velocity has no influence on the transferred charge density $\Delta\sigma$ under the constant displacement (Figure 5d).

Because the essence in the working mechanism of the sliding-TENG is the cycled switching between the separation and full contact of the opposite tribo-charges, there should be little electricity generated in the following two cases: (1) If the sliding motion does not result in the change of the contact area between two plates, for example, if a smaller plate slides inside the perimeter of a larger plate at all time, then little output can be measured, as shown in Figure S3 in the Supporting Information. This is because there is no polarization generated in this case. (2) If the two plates are not fully in tight contact

dx.doi.org/10.1021/nl400738p | Nano Lett. 2013, 13, 2226−2233

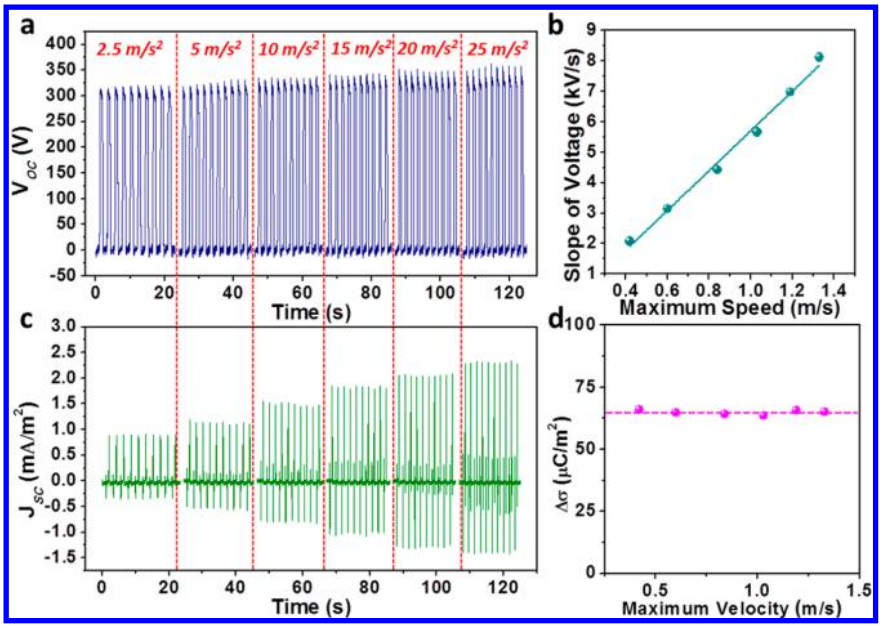

Figure 5. Influence of the sliding velocity (acceleration) on the electrical outputs. (a) The open-circuit voltage (V_{OC}) under six different sliding accelerations (which correspond to different maximum velocity). (b) The plot of the maximum slope of the voltage change versus the maximum velocity. The dots are measured value and the line is the fitted result. (c) The short-circuit current density (J_{SC}) under six different sliding accelerations. (d) The plot of the measured transferred charge density ($\Delta\sigma$) versus the maximum velocity.

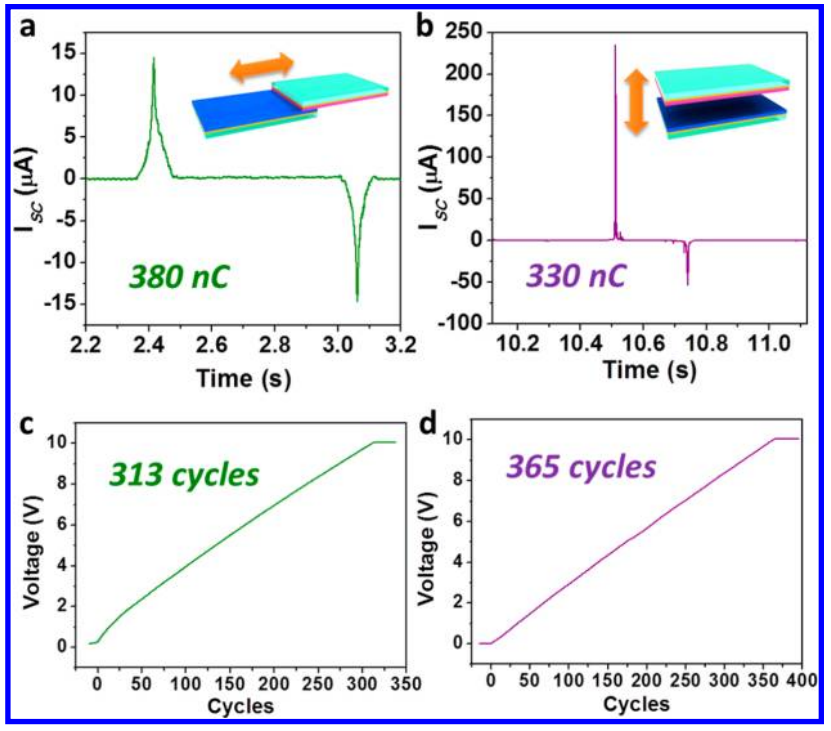

Figure 6. Comparison between the TENGs of the planar-sliding mode and the vertical-touching mode. (a,b) The profiles of the short-circuit current (I_{SC}) peaks within one cycle: (a) the TENG of the planar-sliding mode, and (b) the TENG of the vertical-touching mode. The insets are the schematics showing the corresponding working modes. The amounts of transferred charges from a single displacement have been marked in the figures. (c,d) Capacitors of 22 μF were charged from 0 to 10 V by the TENGs of the two modes, respectively: (c) the TENG of the planar-sliding mode, which takes 313 displacement cycles, and (d) the TENG of the vertical-touching mode, which takes 365 displacement cycles.

with each other at the overlapping position, there is always a vertical gap distance between them, which results in two cases. In one case, little triboelectric charges are generated. The other case is that if there are triboelectric charges on the plates the gap between them in the vertical direction quickly decays the strength of electrostatic interaction, resulting in a reduced output. As shown in Figure S4 in the Supporting Information, when we gradually increase the vertical distance between the two plates of the TENG from 0 to 2 mm, the output voltage, current, and transferred charges all quickly decay to zero.

The working principle of this in-plane-separation based TENG is essentially similar to that of the existing vertical-

dx.doi.org/10.1021/nl400738p | Nano Lett. 2013, 13, 2226−2233

separation based TENG. However, the characteristics of the electrical output differ a lot. As shown in the experimental comparison of the TENGs in these two modes with the same materials and dimensions (Figure 6), the short-circuit current of the TENG in the planar-sliding mode has a much smaller peak value (~15 μA) but a longer pulse (Figure 6a), compared to a much larger peak value of (~240 μA) but a much shorter pulse by the TENG in the vertical-touching mode (Figure 6b). This results from the difference in the charge separation process: in the planar-sliding mode, the length of the effective displacement is very large (71 mm in this experimental case), thus the charge transfer takes much longer time, while in the vertical-touching mode, the effective displacement length is much smaller (less than 1 mm), resulting in a much faster charge flow (Figure S5 in the Supporting Information). Thus, the sliding-TENG should generally deliver a smaller peak instantaneous power than the TENG of the vertical-touching mode. However, as for the total amount of charges flowing through the external load for each displacement, the TENG of the planar-sliding mode delivered a larger value (380 nC) than the TENG of the vertical-touching mode (330 nC), which stands for a higher triboelectric charge density on the polymeric surface. The probable reason is that the lateral sliding between the two polymeric surfaces provides much more friction, thus could more effectively facilitate the triboelectrification than the vertical-touching mode.

As a power source, the electricity generated by the TENGs needs to be regulated and stored in an energy storage device before powering electronic devices. It is the total amount of charges, rather than the peak current, that acts as the key factor for the efficiency of charging an energy storage device. As shown in Figure 6c,d, the TENGs in these two modes were used to charge a capacitor of 22 μF. It took 313 cycles for the sliding-TENG to charge such an empty capacitor to 10 V, while it took 365 cycles for the TENG in the vertical-touching mode. So, the proposed TENG in the planar-sliding mode shows the superiority when combined with an energy storage device.

Besides the above advantage, this new TENG in the planar-sliding mode has several other unique advantages. First, this novel design of TENG does not need a gap between the two plates. Thus it will be unnecessary to have elastic supporting components (such as springs) between the two plates[20,22] to ensure the effective charge separation. This brings up a lot of convenience in packaging the TENG device. Second, there is no need for a large amount of mechanical energy input to trigger this type of TENG, which can help to improve the energy harvesting efficiency. The mechanical energy only needs to overcome the work done by the sliding friction between the two plates. Third, this TENG is simple in structure, easy in fabrication, compact in volume, stable in performance, cost-effective, and robust. With these great advantages, such in-plane charge-separation-based TENGs can harvest mechanical energies in the form of relative sliding that are supplied by many different working configurations, for example, the relative rotation of two contacting plates, the vibration of the piston, the rotation of the axis to its tube, and so on. Besides, those mechanical energies that can drive the relative sliding between two objects can also be harvested using this principle of in-plane charge-separation-based TENG, which can greatly expand the application of this type of TENG to scavenge mechanical energy from wind power, oceanic wave, human activities, and so on.

In summary, we have demonstrated a newly designed triboelectric nanogenerator based on the in-plane separation of triboelectric charges. Through converting the mechanical energy in the planar-sliding motion, the TENG delivered an open-circuit voltage of 1300 V and a short-circuit current density of 4.1 mA/m^2 with the maximum instantaneous power of 5.3 W/m^2, which was able to drive hundreds of electronic devices (such as LEDs) simultaneously. The dependence of the electrical outputs on the sliding motion has been systematically studied, both theoretically and experimentally. Compared with the existing vertical-touching based TENG, the sliding-based TENG drives a larger amount of charges through the external load in each cycle, which is more efficient in charging an energy storage device. This study opens up a new direction in triboelectric nanogenerators and paves the way for a lot of potential applications in harvesting mechanical energy from human activities, rotating tires, mechanical equipment, wind power, ocean waves, and so forth. Furthermore, with the relationship between the electrical output and the sliding motion being calibrated the sliding-based TENG could potentially be used as a self-powered displacement/speed/acceleration sensor.

Methods. *The Fabrication of the Nanowire Array on the Surface of PTFE Film.* The 50 μm thick PTFE film was first washed with menthol, isopropyl alcohol, and deionized water, consecutively, and then blown dry with nitrogen. Subsequently, a thin film of Au with a thickness of 10 nm was sputtered onto the PTFE surface as the mask for the etching process. Then the ICP reactive ion etching was used to produce the aligned nanowires on the surface. Specifically, Ar, O_2, and CF_4 gases were introduced in the ICP chamber with the flow ratio of 15.0, 10.0, and 30.0 sccm, respectively. One power source of 400 W was used to generate a large density of plasma and the other power of 100 W was used to accelerate the plasma ions. The PTFE film was etched for 40 s to get the nanowire array with an average length of ~1.5 μm.

The Fabrication of the Planar-Sliding-Based TENG. A piece of etched PTFE film and a piece of cleaned polyamide 6,6 (Nylon) film, both with the dimensions of 71 mm × 50 mm, were deposited a layer of Cu film with the thickness of 150 nm on the back. Then, the conducting copper wires were connected to the two electrodes respectively as the leads. Finally, the two pieces of films were carefully taped to two glass slides of the same dimensions with the electrode side facing the glass slides. During the operation, the PTFE covered plate was fastened to a stationary stage, and the Nylon-covered plate was bonded to a flat rail guide, which is in parallel and connected to a linear motor to trigger the sliding motion.

The Fabrication of the Vertical-Touching-Based TENG. The fabrication of the two plates for the TENG was the same as the fabrication of the planar-sliding based TENG. Two pieces of cast acrylic sheets with the thickness of 3/8 in. were prepared as the substrates with the dimensions of 3 in. × 3 in. Four half-through holes were drilled at the corners of each acrylic sheet for spring installation. The two plates were taped in the center of the acrylic sheet. Then, four springs were installed in the holes to connect the two substrates together, leaving a gap of ~1 mm between the PTFE surface and Nylon surface.

■ ASSOCIATED CONTENT

Supporting Information

More detailed information about the mechanism of the sliding TENG, the change rate of voltage at different velocity, the

dx.doi.org/10.1021/nl400738p | Nano Lett. 2013, 13, 2226−2233

output of the TENG with no in-plane charge separation during sliding, the influence of the vertical gap distance between the two plates, and the comparison of the charge transfer behavior of the TENGs under the two different modes. This material is available free of charge via the Internet at http://pubs.acs.org.

AUTHOR INFORMATION

Corresponding Author

*E-mail: zlwang@gatech.edu.

Author Contributions

#S.W. and L.L. contributed equally.

Notes

The authors declare no competing financial interest.

ACKNOWLEDGMENTS

Research was supported by Airforce, U.S. Department of Energy, Office of Basic Energy Sciences under Award DEFG02-07ER46394, NSF, and the Knowledge Innovation Program of the Chinese Academy of Sciences (Grant KJCX2-YW-M13). Patents have been filed to protect the reported technologies.

REFERENCES

(1) Wang, Z. L.; Zhu, G.; Yang, Y.; Wang, S. H.; Pan, C. F. *Mater. Today* **2012**, *15*, 532−543.
(2) Wang, Z. L.; Song, J. H. *Science* **2006**, *312*, 242−246.
(3) Oregan, B.; Gratzel, M. *Nature* **1991**, *353*, 737−740.
(4) Tian, B. Z.; Zheng, X. L.; Kempa, T. J.; Fang, Y.; Yu, N. F.; Yu, G. H.; Huang, J. L.; Lieber, C. M. *Nature* **2007**, *449*, 885−U888.
(5) Dresselhaus, M. S.; Chen, G.; Tang, M. Y.; Yang, R. G.; Lee, H.; Wang, D. Z.; Ren, Z. F.; Fleurial, J. P.; Gogna, P. *Adv. Mater.* **2007**, *19*, 1043−1053.
(6) Yang, Y.; Wang, S. H.; Zhang, Y.; Wang, Z. L. *Nano Lett.* **2012**, *12*, 6408−6413.
(7) Wang, Z. L. *Adv. Mater.* **2012**, *24*, 280−285.
(8) Xu, S.; Qin, Y.; Xu, C.; Wei, Y. G.; Yang, R. S.; Wang, Z. L. *Nat. Nanotechnol.* **2010**, *5*, 366−373.
(9) Miao, P.; Mitcheson, P. D.; Holmes, A. S.; Yeatman, E. M.; Green, T. C.; Stark, B. H. *Microsyst. Technol.* **2006**, *12*, 1079−1083.
(10) Mitcheson, P. D.; Miao, P.; Stark, B. H.; Yeatman, E. M.; Holmes, A. S.; Green, T. C. *Sens. Actuators, A* **2004**, *115*, 523−529.
(11) Chang, C. E.; Tran, V. H.; Wang, J. B.; Fuh, Y. K.; Lin, L. W. *Nano Lett.* **2010**, *10*, 726−731.
(12) Wang, X. D.; Song, J. H.; Liu, J.; Wang, Z. L. *Science* **2007**, *316*, 102−105.
(13) Xue, X. Y.; Wang, S. H.; Guo, W. X.; Zhang, Y.; Wang, Z. L. *Nano Lett.* **2012**, *12*, 5048−5054.
(14) Beeby, S. P.; Torah, R. N.; Tudor, M. J.; Glynne-Jones, P.; O'Donnell, T.; Saha, C. R.; Roy, S. *J. Micromech. Microeng.* **2007**, *17*, 1257−1265.
(15) Sari, I.; Balkan, T.; Kulah, H. *Sens. Actuators, A* **2008**, *145*, 405−413.
(16) Castle, G. S. P. *J. Electrostat.* **1997**, *40−1*, 13−20.
(17) McCarty, L. S.; Whitesides, G. M. *Angew. Chem., Int. Ed.* **2008**, *47*, 2188−2207.
(18) Fan, F. R.; Lin, L.; Zhu, G.; Wu, W. Z.; Zhang, R.; Wang, Z. L. *Nano Lett.* **2012**, *12*, 3109−3114.
(19) Fan, F. R.; Tian, Z. Q.; Wang, Z. L. *Nano Energy* **2012**, *1*, 328−334.
(20) Wang, S. H.; Lin, L.; Wang, Z. L. *Nano Lett.* **2012**, *12*, 6339−6346.
(21) Zhu, G.; Lin, Z.-H.; Jing, Q. S.; Bai, P.; Pan, C. F.; Yang, Y.; Zhou, Y. S.; Wang, Z. L. *Nano Lett.* **2013**, *13*, 847−853.
(22) Zhu, G.; Pan, C. F.; Guo, W. X.; Chen, C. Y.; Zhou, Y. S.; Yu, R. M.; Wang, Z. L. *Nano Lett.* **2012**, *12*, 4960−4965.
(23) Zhong, J. W.; Zhong, Q. Z.; Fan, F. R.; Zhang, Y.; Wang, S. H.; Hu, B.; Wang, Z. L.; Zhou, J. *Nano Energy* **2012**, DOI: 10.1016/j.nanoen.2012.11.015.
(24) Zhang, X. S.; Han, M. D.; Wang, R. X.; Zhu, F. Y.; Li, Z. H.; Wang, W.; Zhang, H. X. *Nano Lett.* **2013**, *13* (3), 1168−1172.
(25) Diaz, A. F.; Felix-Navarro, R. M. *J. Electrostat.* **2004**, *62*, 277−290.
(26) Fang, H.; Wu, W. Z.; Song, J. H.; Wang, Z. L. *J. Phys. Chem. C* **2009**, *113*, 16571−16574.
(27) Saurenbach, F.; Wollmann, D.; Terris, B. D.; Diaz, A. F. *Langmuir* **1992**, *8*, 1199−1203.